Demonstration of the three-photon de Broglie wavelength by projection measurement

B. H. Liu,[1] F. W. Sun,[1] Y. X. Gong,[1] Y. F. Huang,[1] Z. Y. Ou,[1,2,*] and G. C. Guo[1]

[1]*Key Laboratory of Quantum Information, University of Science and Technology of China, CAS, Hefei, 230026, People's Republic of China*

[2]*Department of Physics, Indiana University-Purdue University Indianapolis, 402 North Blackford Street, Indianapolis, Indiana 46202, USA*

(Received 31 October 2006; revised manuscript received 26 December 2007; published 12 February 2008)

Two schemes of projection measurement are realized experimentally to demonstrate the de Broglie wavelength of three photons without the need for a maximally entangled three-photon state (the NOON state). The first scheme is based on a proposal by [Wang and Kobayashi, Phys. Rev. A **71**, 021802(R) (2005)] that utilizes a couple of asymmetric beam splitters while the second one applies the general method of NOON-state projection measurement to a three-photon case. Quantum interference of three photons is responsible for projecting out the unwanted states, leaving only the NOON-state contribution in these schemes of projection measurement. A detailed multimode analysis is made to account for imperfect situations in the experiments.

DOI: 10.1103/PhysRevA.77.023815 PACS number(s): 42.50.Dv, 42.25.Hz, 42.50.St, 03.65.Ta

I. INTRODUCTION

The photonic de Broglie wavelength of a multiphoton state is the equivalent wavelength of the whole system when all the photons in the system act as one entity. Early work by Jacobson *et al.* [1] utilized a special beam splitter that sends a whole incident coherent state to either one of the outputs thus creating a Schrödinger-cat-like state. The equivalent de Broglie wavelength in this case was shown to be $\lambda/\langle n\rangle$ with $\langle n\rangle$ as the average photon number of the coherent state. Such a scheme can be used in precision phase measurement to achieve the so-called Heisenberg limit [2–5] of $1/\langle n\rangle$ in phase measurement uncertainty.

Perhaps, the easiest way to demonstrate the de Broglie wavelength is to use a maximally entangled photon number state or the so-called NOON state of the form [4–6]

$$|\mathrm{NOON}\rangle = \frac{1}{\sqrt{2}}(|N\rangle_1|0\rangle_2 + |0\rangle_1|N\rangle_2), \tag{1}$$

where 1 and 2 denote two different modes of an optical field. The N photons in this state stick together either all in mode 1 or all in mode 2. Indeed, if we recombine modes 1 and 2 and make an N-photon coincidence measurement, the coincidence rate is proportional to

$$R_N \propto 1 + \cos(2\pi N\Delta/\lambda), \tag{2}$$

where Δ is the path difference between the two modes and λ is the single-photon wavelength. Equation (2) shows an equivalent de Broglie wavelength of λ/N for N photons.

The NOON state of the form in Eq. (1) for the $N=2$ case was realized with two photons from a parametric down-conversion process, which led to the demonstrations of the two-photon de Broglie wavelength [7,8]. For $N>2$, however, it is not easy to generate the NOON state. The difficulty lies in the cancellation of all the unwanted terms of $|k,N-k\rangle$ with $k\neq 0,N$ in an arbitrary N-photon entangled state of

$$|\Phi_N\rangle = \sum_{k=0}^{N} c_k|k,N-k\rangle. \tag{3}$$

A number of schemes have been proposed [9–11] and demonstrated [12,13] which were based on some sort of multiphoton interference scheme for the cancellation.

Without exceptions, the proposed and demonstrated schemes [9–13] for NOON-state generation rely on multiphoton coincidence measurement for revealing the phase-dependent relation in Eq. (2). Since coincidence measurement is a projective measurement, it may not respond to all the terms in Eq. (3). Indeed, Wang and Kobayashi [14] applied this idea to a three-photon state and found that only the NOON-state part of Eq. (3) contributes to a specially designed coincidence measurement scheme with asymmetric beam splitters. The coincidence rate shows the signature dependence in the form of Eq. (2) on the path difference for the three-photon de Broglie wavelength. Another projective scheme was recently proposed by Sun *et al.* [15] and realized experimentally by Sun *et al.* [16] for four photons and by Resch *et al.* [17] for six photons. This scheme directly projects an arbitrary N-photon state of the form in Eq. (3) onto an N-photon NOON state and thus can be scaled up to an arbitrary N-photon case.

In this paper, we will apply the two projective schemes to the three-photon case. The three-photon state is produced from two pairs of photons in parametric down-conversion by gating on the detection of one photon among them [18]. We find that because of the asymmetric beam splitters, the scheme by Wang and Kabayashi [14] has some residual single-photon effect under a less than perfect situation while the NOON-state projection scheme cancels all lower-order effects regardless the situation.

The paper is organized as follows: in Sec. II, we will discuss the scheme by Wang and Kobayashi [14] and its experimental realization. In Sec. III, we will investigate the NOON-state projection scheme for the three-photon case and implement it experimentally. In both sections, we will use a more realistic multimode model to cover the imperfect situations. We conclude with a discussion.

*zou@iupui.edu

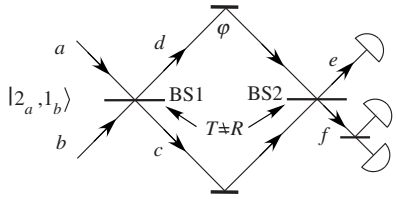

FIG. 1. Arrangement of asymmetric beam splitters of a three-photon interferometer for the demonstration of the three-photon de Broglie wavelength.

II. PROJECTION BY ASYMMETRIC BEAM SPLITTERS

The first scheme for the three-photon case was proposed by Wang and Kobayashi [14], who used two asymmetric beam splitters to cancel the unwanted $|2,1\rangle$ and $|1,2\rangle$ terms. This is a generalization of the two-photon Hong-Ou-Mandel interferometer [7,8,19]. But different from the two-photon case, the state for phase sensing is not a three-photon NOON state since only one unwanted term can be cancelled and there is still another one left there. So a special arrangement has to be made in the second beam splitter to cancel the contribution from the other term. The following gives the details of the scheme.

A. Principle of experiment

We start with a single-mode argument by Wang and Kobayashi. The input state is a three-photon state of $|2\rangle_a|1\rangle_b$. The three photons are incident on an asymmetric beam splitter (BS1) with $T\neq R$ from two sides as shown in Fig. 1. The output state can be easily found from the quantum theory of a beam splitter as [20,21]

$$|\mathrm{BS1}\rangle_{out} = \sqrt{3T^2R}|3_c,0_d\rangle + \sqrt{3TR^2}|0_c,3_d\rangle + \sqrt{T}(T-2R)|2_c,1_d\rangle + \sqrt{R}(R-2T)|1_c,2_d\rangle. \quad (4)$$

When $R=2T=2/3$, the $|1_c,2_d\rangle$ term disappears from Eq. (4) due to three-photon interference and Eq. (4) becomes

$$|\mathrm{BS1}\rangle_{out} = \frac{\sqrt{2}}{3}|3_c,0_d\rangle + \frac{2}{3}|0_c,3_d\rangle - \frac{\sqrt{3}}{3}|2_c,1_d\rangle. \quad (5)$$

But unlike the two-photon case, the $|2_c,1_d\rangle$ term is still in Eq. (5) so that the output state is not a NOON state of the form in Eq. (1).

Now we can arrange a projection measurement to take out the $|2_c,1_d\rangle$ term in Eq. (5). Let us combine c and d with another beam splitter (BS2 in Fig. 1) that has the same transmissivity and reflectivity ($R=2T=2/3$) as the first BS (BS1). Similar to the situation encountered in Eq. (5), $|2_c,1_d\rangle$ will not contribute to the probability $P_3(1_e,2_f)$. So only $|3_c,0_d\rangle$ and $|0_c,3_d\rangle$ in Eq. (5) will contribute. The projection measurement of $P_3(1_e,2_f)$ will cancel the unwanted middle terms like $|2_c,1_d\rangle$ from Eq. (5). Although the coefficients of $|3_c,0_d\rangle$ and $|0_c,3_d\rangle$ in Eq. (5) are not equal, their contributions to $P_3(1_e,2_f)$ are the same after considering the unequal T and R in BS2. So the projection measurement of $P_3(1_e,2_f)$ is responsive only to the three-photon NOON state. Use of an asymmetric beam splitter for the cancellation of $|2_c,1_d\rangle$ was first discussed by Sanaka *et al.* in Fock-state filtering [18].

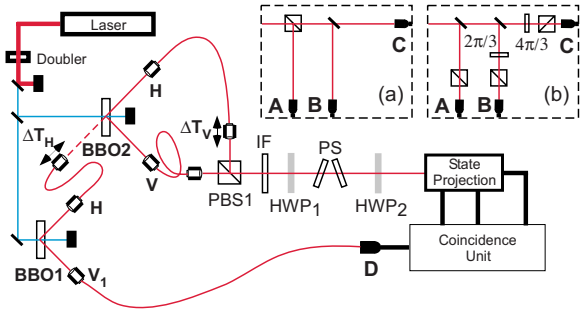

FIG. 2. (Color online) Experimental setup. HWP1 and HWP2 are half-wave plates and are set for different measurements. PS is a phase shifter to introduce phase difference between H and V photons. IF is an interference filter. ΔT_H is the delay between the two H photons, and ΔT_V is the delay between the H photons and the V photon. Insets: (a) arrangement with asymmetric beam splitters by polarization beam splitter (PBS) and (b) the three-photon NOON-state projection.

The above argument can be confirmed by calculating the three-photon coincidence rate $P_3(1_e,2_f)$ directly for the scheme in Fig. 1, which is proportional to [22]

$$P_3(1_e,2_f) = \langle 2_a,1_b|\hat{e}^\dagger\hat{f}^{\dagger 2}\hat{f}^2\hat{e}|2_a,1_b\rangle, \quad (6)$$

with

$$\hat{e} = (\hat{c} + e^{i\varphi}\sqrt{2}\hat{d})/\sqrt{3}, \quad \hat{f} = (e^{i\varphi}\hat{d} - \sqrt{2}\hat{c})/\sqrt{3}, \quad (7)$$

where we introduce a phase φ between c and d. But for the first BS, we have

$$\hat{c} = (\hat{a} + \sqrt{2}\hat{b})/\sqrt{3}, \quad \hat{d} = (\hat{b} - \sqrt{2}\hat{a})/\sqrt{3}. \quad (8)$$

Substituting Eq. (7) into Eq. (6) with Eq. (8), we obtain

$$P_3(1_e,2_f) = \langle 2_a,1_b|\hat{e}^\dagger\hat{f}^{\dagger 2}\hat{f}^2\hat{e}|2_a,1_b\rangle = \frac{32}{81}(1+\cos 3\varphi), \quad (9)$$

which has a dependence on the path difference $\Delta=\varphi\lambda/2\pi$ that is the same as in Eq. (2), but with $N=3$.

B. Experiment

Experimentally, asymmetric beam splitters are realized via polarization projections as shown in Fig. 2 and its inset (a), where a three-photon state of $|2_H,1_V\rangle$ is incident on a combination of two half-wave plates (HWP1, HWP2) and a phase shifter (PS). The first half-wave plate (HWP1) rotates the polarizations of the state $|2_H,1_V\rangle$ by an angle α to $|2_a,1_b\rangle$ with

$$\hat{a}_H = \hat{a}\cos\alpha + \hat{b}\sin\alpha, \quad \hat{a}_V = \hat{b}\cos\alpha - \hat{a}\sin\alpha, \quad (10)$$

where $\cos\alpha=\sqrt{T}=1/\sqrt{3}$ is the amplitude transmissivity of the asymmetric beam splitter. Equations (10) are equivalent to Eqs. (8). The PS, made of birefringent quartz crystals, introduces the phase shift φ between the H and V polarizations. The second half-wave plate (HWP2) makes another rotation of the same angle α for the two phase-shifted polar-

izations and the polarization beam splitter (PBS) in the inset (a) of Fig. 2 finishes the projection required by Eqs. (7).

The three-photon polarization state of $|2_H,1_V\rangle$ is prepared by using two type-II parametric down-conversion processes shown in Fig. 2. This scheme was first constructed by Liu *et al.* [23] to demonstrate controllable temporal distinguishability of three photons. When the delay between the two H photons is zero, we have the state of $|2_H,1_V\rangle$. Specifically in this scheme, two 2-mm-long β barium borate (BBO) crystals are pumped by two UV pulses from a common source of a frequency-doubled Ti:sapphire laser. The mode-locked Ti:sapphire laser is operating at 780 nm and has a pulse duration of 150 fs. The UV pump pulses at 390 nm after frequency doubling have a bandwidth of 3 nm, a repetition rate of 76 MHz, and an average power of 200 mW at BBO1 and 100 mW at BBO2. The pump fields are mildly focused with a beam size of 0.5 mm at the crystals. The two BBO crystals are cut for type-II parametric down-conversion ($\theta=42.62°$, $\varphi=30°$) at degenerate frequency. The θ angle is slightly adjusted so that the two down-converted fields at 780 nm are beam-like [24]. This geometry will ensure an optimum down-conversion rate in a certain direction.

The H photon from BBO1 is coupled to the H polarization mode of BBO2 while the other V photon is detected by detector D and serves as a trigger. Although it is not crucial, the alignment of the H photon from BBO1 to the H polarization mode of BBO2 will increase the production rate of the state $|2_H,1_V\rangle$. To achieve a good mode match, the H photon from BBO1 is first coupled into a single-mode polarization-preserving fiber. The output of the fiber is collimated and then mildly focused so that it has the same spot size as the pump field at BBO2. The alignment of H photon from BBO1 to BBO2 is achieved by coupling the H photons from both BBO1 and BBO2 into a common single-mode polarization preserving fiber. The V photon from BBO2 is coupled to another single-mode polarization-preserving fiber. The outputs of the two fibers, after collimation, are then combined by a polarization beam splitter (PBS1). The combined fields pass through an interference filter (IF) with 3 nm bandwidth and then go through an assembly of HWP1, PS, and HWP2 to form a three-photon polarization interferometer. There are two schemes of projection measurement. In this section, we deal with the first scheme in inset (a) of Fig. 2, which consists of a PBS for projection and three detectors (A, B, C, EG&G SPCM-AQR-15) for measuring the quantity $P_3(1_e,2_f)$ in Eq. (6) by three-photon coincidence (EG&G ORTEC CO4020). To realize the transformation in Eqs. (7) and (8), HWP1 and HWP2 are set to rotate the polarization by $\alpha=\cos^{-1}(1/\sqrt{3})=54.7°$. In order to obtain an input state of $|2_H,1_V\rangle$ to the interferometer, we need to gate the three-photon coincidence measurement on the detection at detector D. In this way, we ensure that the two H photons come from two crystals separately. Otherwise, we will have an input state of $|2_H,2_V\rangle$. The delay (ΔT_H in Fig. 2) between the two H photons from BBO1 and BBO2 and the delay (ΔT_V in Fig. 2) between the H and V photons are adjusted to ensure that the three photons are indistinguishable in time. This is confirmed by the photon-bunching effect of the two H photons [23] and a generalized Hong-Ou-Mandel effect for three photons [18].

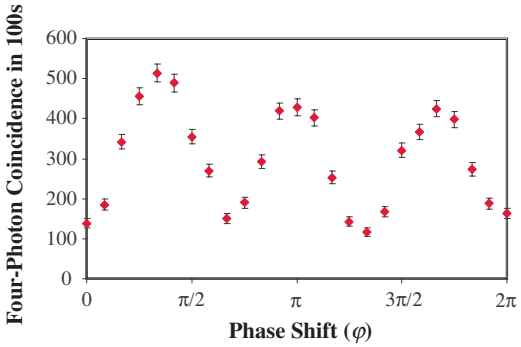

FIG. 3. (Color online) Raw experimental data for projection measurement with asymmetric beam splitters.

The four-photon coincidence count among $ABCD$ detectors is measured as a function of the phase shift φ. The raw experimental data are shown in Fig. 3. The data are gathered in 100 s for each point, and the error bars are one standard deviation. However, there is a contribution from backgrounds due to three pairs of photons. The three-pair contribution can be estimated from the measured single and two-photon rates at each point via the formula

$$\begin{aligned} P_4(\text{3-pair}) = {} & P_2(AB)P_1(C)P_1(D) + P_2(AC)P_1(B)P_1(D) \\ & + P_2(AD)P_1(C)P_1(B) + P_2(BC)P_1(A)P_1(D) \\ & + P_2(BD)P_1(C)P_1(A) + P_2(CD)P_1(A)P_1(B) \\ & + P_{\text{pair}}[P_2(AB)P_2(CD) + P_2(AC)P_2(BD) \\ & + P_2(AD)P_2(CB)]. \end{aligned} \tag{11}$$

This formula is based on the fact that pair generation in parametric down-conversion is random so that the three-pair probability is a product of the single-pair probabilities. Four-photon coincidence is from simultaneous photon detection in four detectors. So for three-pair contributions, the four detectors may detect one pair and one from each of the other two pairs or simply two pairs with the third pair undetected. For the former case, there are six possible arrangements such as $P_2(AB)P_1(C)P_1(D)$ in Eq. (11) with $P_2(AB)$ being two-photon coincidence probability from detectors A and B and $P_1(C),P_1(D)$ being the single-photon detection probability from C and D, respectively. For the latter case, it is $[P_2(AB)P_2(CD)+P_2(AC)P_2(BD)+P_2(AD)P_2(CB)]P_{\text{pair}}$ in Eq. (11). P_{pair} is the single-pair probability in each pulse and is calculated as $P_1(D)/\alpha_D$ with α_D as the overall efficiency of detector D. Note that $P_1(C)P_1(D)=P_2^{acc}(CD)$ is also known as the accidental two-photon probability from two pairs of down-converted photons. Background contributions are calculated using Eq. (11) for each data point and are plotted in Fig. 4.

The experimental result after background subtraction and power correction (monitored by counts from detector D) is shown in Fig. 5, which clearly shows a $\cos 3\varphi$ dependence except the unbalanced minima and maxima, which indicates an extra $\cos\varphi$ dependence. Indeed, the data fit well to the function

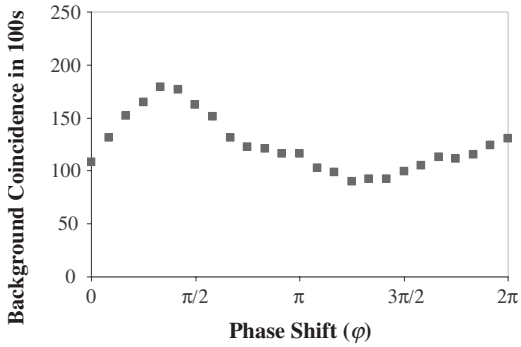

FIG. 4. Background contributions from three-pair events. Each point is calculated by Eq. (11) from the measured rates for one detector and two detectors.

$$P_4 = P_{40}(1 + \mathcal{V}_3 \cos 3\varphi + \mathcal{V}_1 \cos \varphi), \tag{12}$$

with $P_{40}=(184\pm18)/100$ s, $\mathcal{V}_3=(85\pm12)\%$, and $\mathcal{V}_1=(5\pm1)\%$. The χ^2 of the fit is 30 and is comparable to the number of data of 25, indicating a mostly statistical cause for the error.

The appearance of the cos φ term in Eq. (12) is an indication that the cancellation of the $|2_c,1_d\rangle$ and $|1_c,2_d\rangle$ terms is not complete in Eqs. (4) and (9) and the residuals mix with the $|3_c,0_d\rangle$ and $|0_c,3_d\rangle$ terms to produce the cos φ term. This imperfect cancellation is not a result of wrong T,R values, but is due to temporal-mode mismatch among the three photons in the input state of $|2_H,1_V\rangle$. To account for this mode mismatch, we resort to a multimode model of the parametric down-conversion process.

C. Multimode analysis of a three-photon interferometer with asymmetric beam splitters

We start by finding a multimode description of the quantum state from two parametric down-conversion processes. Since the first one serves as the input to the second one, we need the evolution operator for the process, which was first dealt with by Ghosh *et al.* [25] and later by Ou [26] and by Grice and Walmsley [27]. In general, the unitary evolution operator for a weakly pumped type-II process is given by

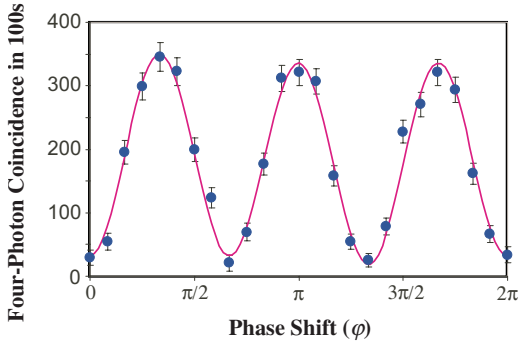

FIG. 5. (Color online) Four-photon coincidence after background subtraction as a function of single-photon phase φ. The data are least-squares-fitted to $P_{40}(1+\mathcal{V}_3\cos 3\varphi+\mathcal{V}_1\cos\varphi)$ with $\mathcal{V}_3=(85\pm12)\%$ and $\mathcal{V}_1=(5\pm1)\%$.

$$\hat{U} = 1 + \eta \int d\omega_1 d\omega_2 \Phi(\omega_1,\omega_2)\hat{a}_H^\dagger(\omega_1)\hat{a}_V^\dagger(\omega_2), \tag{13}$$

where η is some parameter that is proportional to the pump strength and nonlinear coupling. For simplicity without losing generality, we assume that the two processes are identical and are governed by the evolution operator in Eq. (13). Furthermore, we assume the symmetry relation $\Phi(\omega_1,\omega_2)=\Phi(\omega_2,\omega_1)$, which is in general not satisfied, but can be achieved with some symmetrizing tricks [28,29]. So for the first process, because the input is vacuum, we obtain the output state as

$$|\Psi_1\rangle = \hat{U}|\text{vac}\rangle = |\text{vac}\rangle + \eta \int d\omega_1 d\omega_2 \Phi(\omega_1,\omega_2)\hat{a}_H^\dagger(\omega_1)\hat{a}_V^\dagger(\omega_2) \times |\text{vac}\rangle. \tag{14}$$

The second crystal has the state of $|\Psi_1\rangle$ as its input. So after the second crystal, the output state becomes

$$\begin{aligned}|\Psi_2\rangle &= \hat{U}|\Psi_1\rangle \\ &= \cdots + \eta^2 \int d\omega_1 d\omega_2 d\omega_1' d\omega_2' \\ &\quad \times \Phi(\omega_1,\omega_2)\Phi(\omega_1',\omega_2')\hat{a}_H^\dagger(\omega_1')\hat{a}_V^\dagger(\omega_2')\hat{a}_H^\dagger(\omega_1)\hat{a}_{V_1}^\dagger(\omega_2) \\ &\quad \times |\text{vac}\rangle,\end{aligned} \tag{15}$$

where V_1 and V denote the two nonoverlapping vertical polarization modes from the first and second crystals, respectively. Here we only keep the four-photon term. Although there are other four-photon terms in the $|\Psi_2\rangle$ state corresponding to two-pair generation from one crystal alone, they will not contribute to what we are going to calculate. So we omit them in Eq. (15).

The field operators at the four detectors are given by

$$\hat{E}_A(t) = \tau_1\hat{E}_H(t) + \rho_1\hat{E}_V(t), \tag{16}$$

$$\hat{E}_B(t) = [\tau_2\hat{E}_V(t) + \rho_2\hat{E}_H(t)]/\sqrt{2} + \cdots = \hat{E}_C(t),$$

with $\tau_1=(1-2e^{i\varphi})/3$, $\tau_2=(e^{i\varphi}-2)/3$, and $\rho_1=-\rho_2=\sqrt{2}(1+e^{i\varphi})/3$. Here we used relations that are equivalent to Eqs. (7) and (8) to establish the connection between the field operators $\hat{E}_A,\hat{E}_B,\hat{E}_C$ and $\hat{E}_H,\hat{E}_V$. For detector D, we have

$$\hat{E}_D(t) = \hat{E}_{V_1}(t). \tag{17}$$

Here

$$\hat{E}_k(t) = \frac{1}{\sqrt{2\pi}}\int d\omega\, \hat{a}_k(\omega)e^{-i\omega t} \quad (k=H,V,V_1). \tag{18}$$

The four-photon coincidence rate of $ABCD$ is proportional to a time integral of the correlation function

$$\Gamma^{(4)}(t_1,t_2,t_3,t_4) = \langle\Psi_2|\hat{E}_D^\dagger(t_4)\hat{E}_C^\dagger(t_3)\hat{E}_B^\dagger(t_2)\hat{E}_A^\dagger(t_1)\hat{E}_A(t_1)\hat{E}_B(t_2) \times \hat{E}_C(t_3)\hat{E}_D(t_4)|\Psi_2\rangle. \tag{19}$$

It is easy to first evaluate $\hat{E}_A(t_1)\hat{E}_B(t_2)\hat{E}_C(t_3)\hat{E}_D(t_4)$:

$$\hat{E}_A(t_1)\hat{E}_B(t_2)\hat{E}_C(t_3)\hat{E}_D(t_4) = [(HHV+HVH)D\tau_1\tau_2\rho_2 + VHHD\rho_1\rho_2^2]/2 + \cdots, \quad (20)$$

where $H=\hat{E}_H$, $V=\hat{E}_V$, and $D=\hat{E}_D$ for short and we keep the order of arguments $t_1t_2t_3t_4$. We also use an ellipsis ("$\cdots$") to represent the five terms that give zero result when they operate on $|\Psi_2\rangle$. It is now straightforward to calculate the quantity $\hat{E}_A(t_1)\hat{E}_B(t_2)\hat{E}_C(t_3)\hat{E}_D(t_4)|\Psi_2\rangle$, which has the form of

$$\hat{E}_A(t_1)\hat{E}_B(t_2)\hat{E}_C(t_3)\hat{E}_D(t_4)|\Psi_2\rangle = \frac{\eta^2}{2}\{[G(t_1,t_2,t_3,t_4)+G(t_2,t_1,t_3,t_4)+G(t_1,t_3,t_2,t_4) + G(t_3,t_1,t_2,t_4)]\tau_1\tau_2\rho_2 + [G(t_2,t_3,t_1,t_4) + G(t_3,t_2,t_1,t_4)]\rho_1\rho_2^2\}|\text{vac}\rangle, \quad (21)$$

where

$$G(t_1,t_2,t_3,t_4) = g(t_1,t_3)g(t_2,t_4), \quad (22)$$

with

$$g(t,t') \equiv \frac{1}{2\pi}\int d\omega_1 d\omega_2 \Phi(\omega_1,\omega_2)e^{-i(\omega_1 t+\omega_2 t')}.$$

Substituting Eq. (21) into Eq. (19) and carrying out the time integral, we obtain

$$P_4 \propto \int dt_1dt_2dt_3dt_4\Gamma^{(4)}(t_1,t_2,t_3,t_4) = \frac{|\eta|^4}{4}\int d\omega_1 d\omega_2 d\omega_1' d\omega_2'|[\Phi(\omega_1,\omega_2)\Phi(\omega_1',\omega_2') + \Phi(\omega_1,\omega_1')\Phi(\omega_2,\omega_2')](\tau_1\tau_2\rho_2+\rho_1\rho_2^2) + 2\Phi(\omega_1',\omega_2)\Phi(\omega_1,\omega_2')\tau_1\tau_2\rho_2|^2. \quad (23)$$

With τ_1, ρ_1, τ_2, and ρ_2 we can further reduce Eq. (23) to

$$P_4 \propto \frac{2|\eta|^4(17\mathcal{A}+7\mathcal{E})}{243}[1+\mathcal{V}_3\cos 3\varphi + \mathcal{V}_1\cos\varphi], \quad (24)$$

where

$$\mathcal{V}_3 = \frac{8(\mathcal{A}+2\mathcal{E})}{17\mathcal{A}+7\mathcal{E}}, \quad \mathcal{V}_1 = \frac{9(\mathcal{A}-\mathcal{E})}{17\mathcal{A}+7\mathcal{E}} \quad (25)$$

and

$$\mathcal{A} = \int d\omega_1 d\omega_2 d\omega_1' d\omega_2'|\Phi(\omega_1,\omega_2)\Phi(\omega_1',\omega_2')|^2, \quad (26)$$

$$\mathcal{E} = \int d\omega_1 d\omega_2 d\omega_1' d\omega_2'\Phi^*(\omega_1,\omega_2)\Phi^*(\omega_1',\omega_2')\Phi(\omega_1',\omega_2) \times \Phi(\omega_1,\omega_2'). \quad (27)$$

In deducing Eqs. (23)–(27), we used the symmetry relation $\Phi(\omega_1,\omega_2)=\Phi(\omega_2,\omega_1)$.

Obviously, when $\mathcal{A}=\mathcal{E}$, Eq. (24) completely recovers to Eq. (9). In practice, we always have $\mathcal{A}\geq\mathcal{E}$ by the Schwartz inequality. When $\mathcal{E}<\mathcal{A}$, Eq. (24) has the same form as Eq. (12), indicating that the multimode analysis indeed correctly predicts the imperfect cancellation of the $|2_H,1_V\rangle$ and $|2_V,1_H\rangle$ terms in Eqs. (4) and (9). If we use the experimentally measured $\mathcal{V}_3$ and $\mathcal{V}_1$ in Eqs. (25), we will obtain two inconsistent values of $\mathcal{E}/\mathcal{A}$: $(\mathcal{E}/\mathcal{A})_3=0.65$ and $(\mathcal{E}/\mathcal{A})_1=0.87$. This inconsistency is partly due to the slight mismatch of the spatial modes between H and V polarizations in PBS1 (Fig. 2). Indeed, we observed a visibility of $v_1^{obs}=0.98$ in the single-photon interference exhibited in the two-photon coincidence between detectors A and D (although two-photon coincidence is measured, it is really a single-photon interference effect because detector D is used as a trigger). With this imperfection considered, Eqs. (25) are modified as

$$\mathcal{V}_3 = v_1^3\frac{8(\mathcal{A}+2\mathcal{E})}{17\mathcal{A}+7\mathcal{E}}, \quad \mathcal{V}_1 = v_1\frac{9(\mathcal{A}-\mathcal{E})}{17\mathcal{A}+7\mathcal{E}}, \quad (28)$$

where v_1 is the reduced visibility in single-photon interference due to spatial-mode mismatch. With the extra parameter v_1 in Eqs. (28), we obtain a consistent $(\mathcal{E}/\mathcal{A})=0.86$ with $v_1=0.96$. Note that the deduced v_1 is slightly smaller than the observed $v_1^{obs}=0.98$. This discrepancy may be a result of the breakup of the symmetry relation of $\Phi(\omega_1,\omega_2)=\Phi(\omega_2,\omega_1)$ for type-II parametric down-conversion, which is required for the derivation of Eq. (24). Although Eq. (21) covers the case of $\Phi(\omega_1,\omega_2)\neq\Phi(\omega_2,\omega_1)$, the final result is much more complicated than Eqs. (28) and will not be discussed here.

III. NOON-STATE PROJECTION MEASUREMENT

The projection measurement discussed in the previous section relies on the cancellation of some specific terms and therefore cannot be applied to an arbitrary photon number. In the following, we will discuss another projection scheme that can cancel all the unwanted terms at once and thus can be scaled up.

A. Principle of experiment

The NOON-state projection measurement scheme was first proposed by Sun *et al.* [15] and realized by Sun *et al.* [16] for the four-photon case and by Resch *et al.* [17] for the six-photon case. Since it is based on a multiphoton interference effect, it was recently used to demonstrate the temporal distinguishability of an N-photon state [30,31]. Here we will apply it to a three-photon superposition state for the demonstration of three-photon de Broglie wavelength without the NOON state.

The NOON-state projection measurement scheme for the three-photon case is sketched in inset (b) of Fig. 2. In this scheme, the input field is first divided into three equal parts. Then each part passes through a phase retarder that introduces a relative phase difference of $0,2\pi/3$ and $4\pi/3$, respectively between the H and V polarizations. The phase-shifted fields are then projected into the 135° direction by polarizers before being detected by the A, B, and C detectors, respectively. It was shown that the three-photon coincidence rate is proportional to

$$P_3 \propto \frac{1}{18}|\langle \mathrm{NOON}_3|\Phi_3\rangle|^2, \tag{29}$$

where $|\mathrm{NOON}_3\rangle=(|3_H,0_V\rangle-|0_H,3_V\rangle)/\sqrt{2}$ and $|\Phi_3\rangle=c_0|3_H,0_V\rangle+c_1|2_H,1_V\rangle+c_2|1_H,2_V\rangle+c_3|0_H,3_V\rangle$. Note that since $|2,1\rangle$ and $|1,2\rangle$ are orthogonal to the NOON state, their contributions to P_3 are zero. Assuming that $|c_0|=|c_3|=c$ and there is a relative phase of φ between H and V so that $c_0=c$, $c_3=ce^{i3\varphi}$, we obtain from Eq. (29)

$$P_3 \propto \frac{|c|^2}{18}(1-\cos 3\varphi), \tag{30}$$

which is exactly in the form of Eq. (2) with $N=3$, showing the three-photon de Broglie wavelength.

B. Experiment

From Sec. II B, we learned that a state of $|2_H,1_V\rangle$ can be produced with two parametric down-conversion processes. This state will of course give no contribution to the NOON-state projection since it is orthogonal to the NOON state. On the other hand, we can rotate the polarizations by 45°. Then the state becomes [20,21]

$$|\Phi_3\rangle = \sqrt{\frac{3}{8}}(|3_H,0_V\rangle - |0_H,3_V\rangle) + \frac{1}{\sqrt{8}}(|2_H,1_V\rangle - |1_H,2_V\rangle), \tag{31}$$

which has the NOON-state component with $c=\sqrt{3/8}$.

Experimentally, the three-photon state of $|2_H,1_V\rangle$ is prepared in the same way described in Sec. II B and shown in Fig. 2. Different from Sec. II B, the polarizations of the prepared state are rotated 45° by HWP1 to achieve the state in Eq. (31). The phase shifter (PS) then introduces a relative phase difference φ between the H and V polarizations and HWP2 is set at zero before the NOON-state projection measurement is performed [inset (b) of Fig. 2]. As before, a four-photon coincidence measurement among *ABCD* detectors is equivalent to a three-photon coincidence measurement by *ABC* detectors gated on the detection at *D*, which is required for the production of $|2_H,1_V\rangle$.

The four-photon coincidence count among *ABCD* detectors is registered in 200 s as a function of the phase φ (PS).

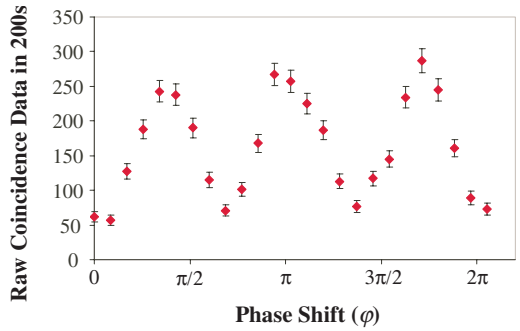

FIG. 6. (Color online) Raw four-photon coincidence data in the NOON-state projection measurement for the demonstration of three-photon de Broglie wavelength.

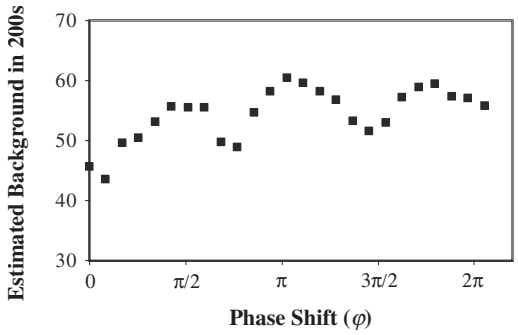

FIG. 7. Estimated background contribution from three pairs of down-conversion photons to four-photon coincidence. Equation (11) is used for the estimation.

The raw data are plotted in Fig. 6. As before, the backgrounds from three pairs must be subtracted from the raw data in order to obtain the true contribution from two pairs of down-conversion. The background is estimated in the same way as in the experiment in Sec. II B and is plotted in Fig. 7. The data after subtraction of background contribution and power correction are plotted in Fig. 8. It clearly shows a sinusoidal dependence on φ with a period of $2\pi/3$. The solid curve is a χ^2 fit to the function of $P_4=P_{40}[1+\mathcal{V}_3\cos 3(\varphi+\varphi_0)]$ with $P_{40}=(103\pm14)/200$ s and $\mathcal{V}_3=(84\pm14)\%$. The χ^2 of the fit is 24.3, which is comparable to a number of data of 25, indicating a good fit with only statistical errors.

The less-than-unit visibility is a result of temporal distinguishability among the three photons produced from two crystals. It can only be accounted for with a multimode model of the state given in Sec. II C. Let us now apply it to the current scheme.

C. Multimode analysis

The input state is the same as Eq. (15). But the field operators are changed to

$$\hat{E}_A(t) = [\hat{E}_+(t) - e^{i\varphi}\hat{E}_-(t)]/\sqrt{6} + \cdots,$$

$$\hat{E}_B(t) = [\hat{E}_+(t) - e^{i\varphi}\hat{E}_-(t)e^{i2\pi/3}]/\sqrt{6} + \cdots,$$

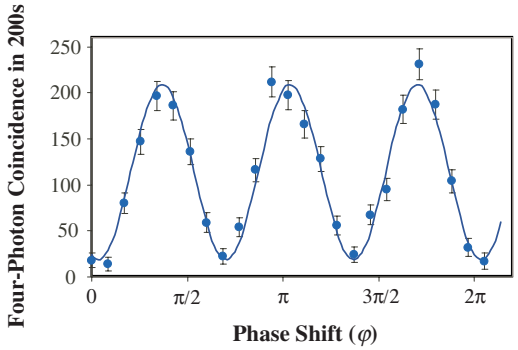

FIG. 8. (Color online) Experimental data after background subtraction for the NOON-state projection measurement. The data are least-squares-fitted to $P_{40}(1+\mathcal{V}_3\cos 3\varphi)$ with $V_3=(84\pm14)\%$.

$$\hat{E}_C(t) = [\hat{E}_+(t) - e^{i\varphi}\hat{E}_-(t)e^{i4\pi/3}]/\sqrt{6} + \cdots, \tag{32}$$

with

$$\hat{E}_+(t) = [\hat{E}_H(t) + \hat{E}_V(t)]/\sqrt{2},$$

$$\hat{E}_-(t) = [\hat{E}_H(t) - \hat{E}_V(t)]/\sqrt{2}, \tag{33}$$

where we omit the vacuum input fields and φ is the phase shift introduced by PS in Fig. 2. The field operator for detector D is the same as Eq. (17).

As in Sec. II C, the four-photon coincidence rate is related to the correlation function in Eq. (19) and we can first evaluate $\hat{E}_A(t_1)\hat{E}_B(t_2)\hat{E}_C(t_3)\hat{E}_D(t_4)$. With the field operators in Eq. (32), we obtained

$$\hat{E}_A(t_1)\hat{E}_B(t_2)\hat{E}_C(t_3)\hat{E}_D(t_4) = \frac{1}{12^{3/2}}(HHVa_1 + HVHa_2 + VHHa_3) + \cdots, \tag{34}$$

with

$$a_1 = 1 + e^{i3\varphi} + 2e^{i(2\varphi+2\pi/3)} + 2e^{i(\varphi+4\pi/3)},$$

$$a_2 = 1 + e^{i3\varphi} + 2e^{i(2\varphi+4\pi/3)} + 2e^{i(\varphi+2\pi/3)},$$

$$a_3 = 1 + e^{i3\varphi} + 2e^{i2\varphi} + 2e^{i\varphi}, \tag{35}$$

where the notations are the same as in Eq. (20) and we used the identity $1+e^{i2\pi/3}+e^{i4\pi/3}=0$. As before, we do not write explicitly the five terms that give zero result when they operate on $|\Psi_2\rangle$. Now we can calculate the quantity $\hat{E}_A(t_1)\hat{E}_B(t_2)\hat{E}_C(t_3)\hat{E}_D(t_4)|\Psi_2\rangle$, which has the form of

$$\hat{E}_A(t_1)\hat{E}_B(t_2)\hat{E}_C(t_3)\hat{E}_D(t_4)|\Psi_2\rangle = \frac{\eta^2}{\sqrt{12^3}}\{[G(t_1,t_2,t_3,t_4) + G(t_2,t_1,t_3,t_4)]a_1 + [G(t_1,t_3,t_2,t_4) + G(t_3,t_1,t_2,t_4)]a_2 + [G(t_2,t_3,t_1,t_4) + G(t_3,t_2,t_1,t_4)]a_3\} \times|\text{vac}\rangle, \tag{36}$$

where $G(t_1,t_2,t_3,t_4)$ is given in Eq. (22). After the time integral, we obtain

$$P_4(\text{NOON}) \propto \frac{|\eta|^4(2\mathcal{A}+\mathcal{E})}{72}(1 + \mathcal{V}_3 \cos 3\varphi), \tag{37}$$

with

$$\mathcal{V}_3(\text{NOON}) = \frac{\mathcal{A}+2\mathcal{E}}{2\mathcal{A}+\mathcal{E}}, \tag{38}$$

where $\mathcal{A}$ and $\mathcal{E}$ are given in Eqs. (26) and (27). Note that the terms such as $\cos 2\varphi, \cos\varphi$ are absent in Eq. (38) even in the nonideal case of $\mathcal{E}<\mathcal{A}$. This is because of the symmetry among the three detectors A, B, and C involved in the three-photon NOON-state projection measurement. When spatial-mode mismatch is considered, the visibility is changed to

$$\mathcal{V}_3(\text{NOON}) = v_1^3\frac{\mathcal{A}+2\mathcal{E}}{2\mathcal{A}+\mathcal{E}}. \tag{39}$$

With v_1 and the quantity $\mathcal{E}/\mathcal{A}$ obtained in Sec. II C, we have $\mathcal{V}_3(\text{NOON})=0.85$, which is close to the observed value of 0.84 ± 0.14 in Sec. III B.

IV. SUMMARY AND DISCUSSION

In summary, we demonstrate the three-photon de Broglie wavelength by using two different schemes of projection measurement without the need for a hard-to-produce NOON state. Quantum interference is responsible for the cancellation of the unwanted terms. The first scheme by asymmetric beam splitters targets specific terms while the second one by NOON-state projection cancels all the unwanted terms at once. We use a multimode model to describe the nonideal situation encountered in the experiment and find good agreement with the experimental results.

Since the scheme by asymmetric beam splitters is only for some specific terms, it cannot be easily scaled up to an arbitrary number of photons, although an extension to the four-photon case is available [32]. The extension of the scheme by NOON-state projection to an arbitrary number of photons is straightforward. In fact, demonstrations with four and six photons have been done with simpler states [16,17].

On the other hand, the scheme of NOON-state projection needs to divide the input fields into N equal parts while the scheme with asymmetric beam splitters requires less partition. So the latter will have a higher coincidence rate than the former. In fact, Figs. 3 and 4 show a ratio of 3.6 between P_{40}. This is consistent qualitatively with the ratio of 4.7 from Eqs. (24) and (37) when $\mathcal{E}=A$. The discrepancy may come from the different collection efficiency resulting from the different geometry in the experimental layouts.

The dependence of the visibility in Eqs. (28) and (38) on the quantity $\mathcal{E}/A$ reflects the fact that the interference effect depends on the temporal indistinguishability of the three photons. From previous studies [15,23,33–35], we learned that the quantity $\mathcal{E}/A$ is a measure of the indistinguishability between two pairs of photons in parametric down-conversion. In our generation of the $|2_H,1_V\rangle$ state, one of the H photons is from another pair of down-converted photons. So to form an indistinguishable three-photon state, we need pair indistinguishability—i.e., $\mathcal{E}/A\rightarrow 1$.

ACKNOWLEDGMENTS

This work was funded by the National Fundamental Research Program of China (Grant No. 2001CB309300), the Innovation funds from Chinese Academy of Sciences, and National Natural Science Foundation of China (Grants No. 60121503 and No. 10404027). Z.Y.O. is also supported by the U.S. National Science Foundation under Grants No. 0245421 and No. 0427647.

[1] J. Jacobson, G. Björk, I. Chuang, and Y. Yamamoto, Phys. Rev. Lett. **74**, 4835 (1995).
[2] W. Heisenberg, Z. Phys. **43**, 172 (1927).
[3] M. J. Holland and K. Burnett, Phys. Rev. Lett. **71**, 1355 (1993).
[4] J. J. Bollinger, W. M. Itano, D. J. Wineland, and D. J. Heinzen, Phys. Rev. A **54**, R4649 (1996).
[5] Z. Y. Ou, Phys. Rev. Lett. **77**, 2352 (1996); Phys. Rev. A **55**, 2598 (1997).
[6] A. N. Boto, P. Kok, D. S. Abrams, S. L. Braunstein, C. P. Williams, and J. P. Dowling, Phys. Rev. Lett. **85**, 2733 (2000); P. Kok, A. N. Boto, D. S. Abrams, C. P. Williams, S. L. Braunstein, and J. P. Dowling, Phys. Rev. A **63**, 063407 (2001).
[7] Z. Y. Ou, X. Y. Zou, L. J. Wang, and L. Mandel, Phys. Rev. A **42**, 2957 (1990).
[8] J. G. Rarity, P. R. Tapster, E. Jakeman, T. Larchuk, R. A. Campos, M. C. Teich, and B. E. A. Saleh, Phys. Rev. Lett. **65**, 1348 (1990).
[9] H. F. Hofmann, Phys. Rev. A **70**, 023812 (2004).
[10] F. Shafiei, P. Srinivasan, and Z. Y. Ou, Phys. Rev. A **70**, 043803 (2004).
[11] B. Liu and Z. Y. Ou, Phys. Rev. A **74**, 035802 (2006).
[12] P. Walther, J. W. Pan, M. Aspelmeyer, R. Ursin, S. Gasparoni, and A. Zeilinger, Nature (London) **429**, 158 (2004).
[13] M. W. Mitchell, J. S. Lundeen, and A. M. Steinberg, Nature (London) **429**, 161 (2004).
[14] H. Wang, and T. Kobayashi, Phys. Rev. A **71**, 021802(R) (2005).
[15] F. W. Sun, Z. Y. Ou, and G. C. Guo, Phys. Rev. A **73**, 023808 (2006).
[16] F. W. Sun, B. H. Liu, Y. F. Huang, Z. Y. Ou, and G. C. Guo, Phys. Rev. A **74**, 033812 (2006).
[17] K. J. Resch, K. L. Pregnell, R. Prevedel, A. Gilchrist, G. J. Pryde, J. L. O'Brien, and A. G. White, Phys. Rev. Lett. **98**, 223601 (2007).
[18] K. Sanaka, K. J. Resch, and A. Zeilinger, Phys. Rev. Lett. **96**, 083601 (2006).
[19] C. K. Hong, Z. Y. Ou, and L. Mandel, Phys. Rev. Lett. **59**, 2044 (1987).
[20] Z. Y. Ou, C. K. Hong, and L. Mandel, Opt. Commun. **63**, 118 (1987).
[21] R. A. Campos, B. E. A. Saleh, and M. C. Teich, Phys. Rev. A **40**, 1371 (1989).
[22] L. Mandel and E. Wolf, *Optical Coherence and Quantum Optics* (Cambridge University Press, New York, 1995).
[23] B. H. Liu, F. W. Sun, Y. X. Gong, Y. F. Huang, Z. Y. Ou, and G. C. Guo, Europhys. Lett. **77**, 24003 (2007).
[24] S. Takeuchi, Opt. Lett. **26**, 843 (2001).
[25] R. Ghosh, C. K. Hong, Z. Y. Ou, and L. Mandel, Phys. Rev. A **34**, 3962 (1986).
[26] Z. Y. Ou, Quantum Semiclassic. Opt. **9**, 599 (1997).
[27] W. P. Grice and I. A. Walmsley, Phys. Rev. A **56**, 1627 (1997).
[28] D. Branning, W. P. Grice, R. Erdmann, and I. A. Walmsley, Phys. Rev. Lett. **83**, 955 (1999).
[29] O. Kuzucu, M. Fiorentino, M. A. Albota, F. N. C. Wong, and F. X. Kärtner, Phys. Rev. Lett. **94**, 083601 (2005).
[30] Z. Y. Ou, Phys. Rev. A **74**, 063808 (2006).
[31] G. Y. Xiang, Y. F. Huang, F. W. Sun, P. Zhang, Z. Y. Ou, and G. C. Guo, Phys. Rev. Lett. **97**, 023604 (2006).
[32] B. H. Liu, F. W. Sun, Y. X. Gong, Y. F. Huang, G. C. Guo, and Z. Y. Ou, Opt. Lett. **32**, 1320 (2007).
[33] Z. Y. Ou, J. K. Rhee, and L. J. Wang, Phys. Rev. A **60**, 593 (1999).
[34] K. Tsujino, H. F. Hofmann, S. Takeuchi, and K. Sasaki, Phys. Rev. Lett. **92**, 153602 (2004).
[35] Z. Y. Ou, Phys. Rev. A **72**, 053814 (2005).